JOURNAL OF BACTERIOLOGY, Mar. 2008, p. 1680–1690 Vol. 190, No. 5
0021-9193/08/$08.00+0 doi:10.1128/JB.01671-07
Copyright © 2008, American Society for Microbiology. All Rights Reserved.

Bioinformatic and Biochemical Evidence for the Identification of the Type III Secretion System Needle Protein of *Chlamydia trachomatis*▽

H. J. Betts,[1] L. E. Twiggs,[1] M. S. Sal,[2] P. B. Wyrick,[2] and K. A. Fields[1]*

Department of Microbiology and Immunology, University of Miami Miller School of Medicine, Miami, Florida 33101,[1] and Department of Microbiology, East Tennessee State University, James H. Quillen College of Medicine, Johnson City, Tennessee 37614[2]

Received 16 October 2007/Accepted 17 December 2007

***Chlamydia* spp. express a functional type III secretion system (T3SS) necessary for pathogenesis and intracellular growth. However, certain essential components of the secretion apparatus have diverged to such a degree as to preclude their identification by standard homology searches of primary protein sequences. One example is the needle subunit protein. Electron micrographs indicate that chlamydiae possess needle filaments, and yet database searches fail to identify a SctF homologue. We used a bioinformatics approach to identify a likely needle subunit protein for *Chlamydia*. Experimental evidence indicates that this protein, designated CdsF, has properties consistent with it being the major needle subunit protein. CdsF is concentrated in the outer membrane of elementary bodies and is surface exposed as a component of an extracellular needle-like projection. During infection CdsF is detectible by indirect immunofluorescence in the inclusion membrane with a punctuate distribution adjacent to membrane-associated reticulate bodies. Biochemical cross-linking studies revealed that, like other SctF proteins, CdsF is able to polymerize into multisubunit complexes. Furthermore, we identified two chaperones for CdsF, termed CdsE and CdsG, which have many characteristics of the *Pseudomonas* spp. needle chaperones PscE and PscG, respectively. In aggregate, our data are consistent with CdsF representing at least one component of the extended *Chlamydia* T3SS injectisome. The identification of this secretion system component is essential for studies involving ectopic reconstitution of the *Chlamydia* T3SS. Moreover, we anticipate that CdsF could serve as an efficacious target for anti-*Chlamydia* neutralizing antibodies.**

Chlamydia trachomatis is one of three members of the genus *Chlamydia*, a group of obligate intracellular gram-negative bacteria, which are a significant risk to human health. The oculogenital pathogen *C. trachomatis*, along with the respiratory pathogen *C. pneumonia* and the zoonotically acquired *C. psittaci*, parasitize the eukaryotic host-cell and develop exclusively within parasitophorous membrane-bound vesicles, termed inclusions (40). This intimate association with the host cell is essential for propagation and survival and is manifested via a biphasic developmental cycle. Infectious yet metabolically inert elementary bodies (EBs) invade target cells and differentiate into the vegetative, noninfectious, metabolically active reticulate bodies (RBs). Replication of RBs occurs within the expanding inclusion in intimate association with the inclusion membrane, and the developmental cycle is completed by the differentiation of RBs back into EBs (40), which later exit the cell by various mechanisms (28).

Despite considerable differences in disease manifestation among the medically important species of *Chlamydia*, basic mechanisms of pathogenesis are clearly conserved. It is clear, for example, that *Chlamydia* spp. express a type III secretion system (T3SS), which is active at all stages of the developmental cycle (18, 26). The T3SS is essential for virulence and is used by a variety of gram-negative human pathogens, including *Yersinia* spp., *Shigella* spp., *Salmonella* spp., pathogenic *Escherichia coli*, and *Pseudomonas* spp., to mediate delivery of bacterial "effector" proteins directly into the host cell cytosol. Effector substrates are typically unique to respective pathogens and are involved in manipulation of host cellular machinery to the advantage of the bacteria (27). In contrast, the type III secretion (T3S) apparatus comprises a functionally conserved multiprotein complex spanning both the bacterial inner and outer membranes and the periplasm. Hence, many of the proteins that constitute the T3S apparatus are highly conserved among species and are easily identified in protein homology searches (20, 21, 57).

Distal to this basal apparatus is an extracellular, needle-like appendage which, like other components of the apparatus, is essential for the translocation of effectors from the bacterial cytosol to the host cell. The needle has been shown to be composed of a single protein that polymerizes upon secretion (25). Numerous studies have demonstrated that deletion or mutation of the gene encoding the needle results in significant attenuation of virulence (31, 53, 55, 56). Experiments using a subcutaneous murine infection model have shown that the *Yersinia pestis* needle protein YscF can serve as a protective antigen, indicating that the needle may have potential in vaccine development (8, 35, 45, 54, 55). In addition to its role as an injectisome component, evidence suggests that the needle is also important in host cell detection and thus regulation of T3S (12, 30, 60). Electron micrographs of the needles from *Yersinia*, *Salmonella* Spi-1, and *Shigella*, comprising the small homologous proteins YscF, PrgI, and MxiH, respectively, reveal straight rigid structures that are very short (approximately 40

* Corresponding author. Mailing address: Department of Microbiology and Immunology, University of Miami Miller School of Medicine, Miami, FL 33101. Phone: (305) 243-6711. Fax: (305) 243-4623. E-mail: Kfields@med.miami.edu.

▽ Published ahead of print on 28 December 2007.

Downloaded from http://jb.asm.org/ on September 23, 2019 by guest

to 80 nm) compared to flagella (7, 25, 34, 55). The crystal structure of monomeric MxiH has recently been solved revealing two extended antiparallel helices reminiscent of the D0 portion of flagellin (11, 12). Deane et al. (12) propose an elegant model for the self-assembly of the MxiH needle where polymerization is mediated by head-to-tail interaction of monomers.

Chaperones within the bacterial cytosol are also important in the process of T3S and are required for stability and efficient secretion of the translocator proteins and some effectors (62). It has also been demonstrated that *Yersinia* YscF and *Pseudomonas* PscF require two distinct chaperones, YscE/YscG and PscE/PscG, respectively, to maintain stability and prevent their premature polymerization within the bacterial cytosol (10, 44, 45). Mutational analysis of PscE and PscG has demonstrated that the formation of heterotrimeric PscE-PscF-PscG is absolutely required for efficient secretion of PscF and full cytotoxicity. Interestingly, the present study also showed that PscE and PscG appear to stabilize each other.

Early on in the field of chlamydial research, spike-like projections were identified and visualized by multiple research groups on the surface of both EBs and RBs (3, 5, 36, 38, 49). Consequently, electron micrographs of these spike-like projections in infected cultures revealed them to form a direct connection between the RB and the inclusion membrane, protruding out into the host cell cytoplasm (37). At the time, it was speculated that these spikes may be involved in the movement of substances in and/or out of the cell (42). Given the identification of T3SS components in all species of *Chlamydia* and the expanding volume of data regarding T3SS function in chlamydiae, it is highly plausible that these spike-like projections represent needle complexes (15, 48, 50, 52, 64). In the present study, we used a bioinformatic and biochemical approach to identify and characterize the needle component of the *C. trachomatis* T3SS, which we have named CdsF. Furthermore, we provide evidence that CT665 and CT667 encode the chaperones CdsE and CdsG, which not only interact with each other and CdsF in a yeast three-hybrid system but also promote the stability of ectopically expressed CdsF.

MATERIALS AND METHODS

Cell culture and organisms. *C. trachomatis* serotype L2 (LGV 434) was used for these studies. Routine propagation was carried out in HeLa 229 epithelial cells (CCL 1.2; American Type Culture Collection, Manassas, VA) maintained in RPMI 1640 supplemented with 10% fetal bovine serum and 10 μg of gentamicin ml^{-1} (Mediatech, Herndon, VA). Cultures were incubated at 37°C in an atmosphere of 5% CO_2 and 95% humidified air, and infections were carried out as previously described (4, 22, 65) in Hanks balanced salt solution (HBSS; Invitrogen, Carlsbad, CA), for 1 h at 37°C. When appropriate, EBs were purified by centrifugation through MD-76R (Mallinckrodt, Inc., St. Louis, MO) density gradients as described previously (4). *Escherichia coli* Novablue (EMD, San Diego, CA) was typically grown at 37°C in either Luria-Bertani (LB) broth or on LB agar plates. Where appropriate, media were supplemented with ampicillin (Sigma, St. Louis, MO) at 100 μg ml^{-1} for plasmid selection or with chloramphenicol (Sigma) at 50 μg ml^{-1} for protein stability assays. *Saccharomyces cerevisiae* MaV203 (Invitrogen) was routinely cultivated on nonselective YPD media at 30°C or on selective media lacking appropriate amino acids for interaction studies.

DNA methods. Specific coding regions were amplified from genomic *C. trachomatis* serovar L2 DNA in an iCycler thermocycler (Bio-Rad, Hercules, CA) using iTaq polymerase (Bio-Rad) and custom oligonucleotide primers synthesized by Integrated DNA Technologies (Coralville, IA). Cloning techniques were performed essentially as described previously (33), and transformations were carried out using chemically competent *E. coli* Novablue according to manufacturer's instructions. All genes were verified by DNA sequencing (Genewiz, South Plainsfield, NJ) of the resulting constructs. To obtain epitope-tagged chimeras containing CdsF, full-length CT666 was amplified with the primers KFCT666-2A (5′-CGCGGATCCTGGCGAGCGGAAGTTGTTCGGC-3′) and KFCT666-1B (5′-TCCGGAATTCTTAACTTCCTTTAACAGCTCTTGCCATGG-3′) or with the primers KFCT666-4A (5′-AAACCGCTCGAGGCGAGCGGAAGTTGTTCGGC-3′) and KFCT666-4B (5′-ATCTGGTACCACTTCCTTTAACAGCTCTTGCCATGG-3′). Primers contained engineered restriction sites (BamHI for KFCT666-2A, EcoRI for KFCT666-1B, XhoI for KFCT666-4A, and KpnI for KFCT666-4B) enabling directional cloning into either BamHI-EcoRI-digested pGEX-3X (GE Healthcare, Piscataway, NJ) or XhoI-KpnI-digested pFLAG-CTC (Sigma) to yield pGST-CdsF and pCdsF-FT, respectively. Expression constructs containing all three coding sequences for CT665, CT666, and CT667 were generated by amplification with the primers KFCT665-3A (5′-AAACCGCTCGAGTTTAATATGGAAAATTCGGCAGCTAAAGG-3′) and KFCT667-1B (5′-ATCTGGTACCATTTAAAGGCCCACCGCTTTTAGC-3′) and mobilization into XhoI-KpnI-digested pFLAG-CTC to create pCdsEFG-FT. Plasmid pCdsFG-FT was similarly generated by insertion of appropriately digested PCR products amplified with primers KFCT666-4A and KFCT667-1B into XhoI-KpnI-digested pFLAG-CTC. Plasmid pCdsEF was derived from pCdsEFG-FT by the deletion of the CT667 coding sequence using a QuikChange site-directed mutagenesis kit (Stratagene, La Jolla, CA). pCdsEFG was amplified with the mutagenic primers 667-bglII-FOR (5′-GCAAGAGCTGTTAAAGGAAGTTAATAAAATAAGAGATGGAGATCTGCAGATTTGGATGTATTTAAAGAAGATTTTGCATTGTTG-3′) and 667-bglII-REV (5′-CAACAATGCAAAATCTTCTTTAAATACATCCAAATCTGCAGATCTCCATCTCTTATTTTATTAACTTCCTTTAACAGCTCTTGC-3′), both containing a BglII restriction site coinciding with the start of CT667. The kit was used according to the manufacturer's instructions to incorporate the BglII site into pCdsEFG. The thermal cycling conditions were 95°C for 1 min, followed by 18 cycles of 95°C for 50 s, 68°C for 50 s, and 68°C for 6 min, followed finally by an extension step of 68°C for 10 min. A QIAprep miniprep kit (Qiagen) was used to isolate plasmid DNA. CT667 was excised by restriction digestion of the plasmid DNA with BglII, followed by gel purification of the linear plasmid using a QIAquick gel purification kit (Qiagen). Subsequent religation with T4 DNA ligase (New England Biolabs, Ipswich, MA) removed CT667 from plasmid pCdsEFG-FT, generating plasmid pCdsEF. The yeast three-hybrid vector pY3HCdsE containing CT665 was derived from plasmid pGBDU-C1 (Clontech). Primers pGBDU665FOR (5′-TACCAAGCATACAATCAACTCCAAGCTTGAAGCAAGCCTCCTGAAAGATTTTAATATGGAAAATTCGGCAGC-3′) and pGBDU665REV (5′-GATTCATAGATCTCTGCAGGTCGACATCGATGGATCCCCCGGGGAATTCCGGTTACACCATTTTACGGTTGATAC-3′) containing 50-bp overlaps homologous to either side of the region encoding the GAL4 activation domain of pGBDU-C1 were used to amplify CT665 from chlamydial DNA purified from EBs. pGBDU-C1 was linearized with EcoRI and cotransformed with the PCR product generated from the primers pGBDU665FOR and PGBDU665REV into *S. cerevisiae* MaV203 using the *S.c.* EasyComp kit (Invitrogen) according to the manufacturer's instructions. Excision repair by MaV203 ligated the PCR product containing CT665 into pGBDU-C1 subsequently deleting the Gal4 activation domain and generating the yeast three-hybrid vector pY3HCdsE.

Protein purification and antibody production. Purified preparations of either glutathione *S*-transferase (GST)-tagged or Flag-tagged CdsF were obtained from extracts of *E. coli* expressing pGST-CdsF or pCdsF-FT, respectively. Strains were cultivated at 37°C in the presence of a 0.1 mM concentration of the inducer IPTG (isopropyl-β-D-thiogalactopyranoside; Sigma), and lysates were generated by using a French press (20,000 lb/in^2) of bacteria suspended in phosphate-buffered saline (PBS; 135 mM NaCl, 2.7 mM KCl, 10 mM Na_2HPO_4, 1.8 mM KH_2PO_4 [pH 8.0]). Cellular debris was removed by centrifugation at 16,000 × *g* for 25 min. GST-tagged CdsF was purified in one step with GST affinity resin in accordance with the manufacturer's instructions (Novagen). Similarly, Flag-tagged CdsF was purified according to manufacturer's instructions (Sigma) by the passage of lysates over a Flag-M2 antibody column, elution with 100 mM glycine (pH 3.5), and neutralization with 1 M Tris (pH 8.0). The purity of the respective proteins was assessed by the resolution of protein samples by sodium dodecyl sulfate-polyacrylamide gel electrophoresis (SDS-PAGE), followed by staining with Coomassie brilliant blue (Pierce, Rockford, IL). Pure preparations were dialyzed into PBS, and protein concentrations were quantitated by a bicinchoninic acid assay (Pierce). Purified GST-CdsF was subsequently used to produce polyclonal antisera by immunization of female New Zealand White rabbits (Proteintech Group, Inc., Chicago, IL). CdsF-specific antibodies were purified from serum by passage over a column of CdsF-FT immobilized on a cyanogen bromide-activated Sepharose 4B agarose resin prepared according to the instructions of the manufacturer

Downloaded from http://jb.asm.org/ on September 23, 2019 by guest

(GE Healthcare). *C. trachomatis* CT665-specific antibodies were generated (Sigma Genosys, The Woodlands, TX) by immunization of female New Zealand White rabbits with a synthetic peptide (NH_2-N-V-Q-S-K-V-Q-T-L-T-S-S-L-R-E-C-CO_2) conjugated to keyhole limpet hemocyanin.

Immunodetection. For immunoblot analyses of *C. trachomatis*-infected HeLa cultures, whole-culture proteins were harvested via cold water lysis as described previously (17). Chlamydial outer membrane complexes (COMCs) were obtained by Sarkosyl extraction of purified EBs essentially as described previously (4, 58). When chlamydial proteins were ectopically expressed in *E. coli*, bacteria were pelleted and suspended in PBS prior to concentration. All proteins were concentrated by the addition of trichloroacetate (Sigma) to 10% (vol/vol) and subsequently solubilized in electrophoresis sample buffer (2.3% [wt/vol] SDS, 5% [vol/vol] β-mercaptoethanol, 25% [vol/vol] glycerol, and 60 mM Tris [pH 6.8]). Proteins were resolved by SDS-PAGE (32) in either 12% (vol/vol) homogeneous or 4 to 20% (vol/vol) gradient (Bio-Rad) polyacrylamide gels and transferred to Immobilon-P (Millipore) in carbonate buffer (10 mM $NaHCO_3$, 3 mM Na_2CO_3, 10% methanol [pH 9.5]). Specific proteins were detected by probing with α-GST-CdsF, α-GST-CdsC (18), α-CT665, α-HT-Scc1 (17), α-HT-CopN (17), α-HT-CdsJ (18), α-MOMP (2), *E. coli*-specific α-Hsp60 (Stressgen Bioreagents, Victoria, British Columbia, Canada), or α-Flag M2 (Sigma) and visualized by using appropriate alkaline phosphatase-conjugated (Sigma) secondary antibodies followed by development with nitroblue tetrazolium–5-bromo-4-chloro-3-indolylphosphate (NBT-BCIP; Gibco-BRL).

Protein localization was assessed by both indirect immunofluorescence of infected HeLa cultures and immunoelectron microscopy of purified *C. trachomatis* EBs. For HeLa cultures, cell monolayers were cultivated as described previously (22) on 12-mm-diameter glass coverslips, infected with *C. trachomatis* L2, and then fixed and permeabilized with methanol at 18 h postinfection. Samples were blocked with 5% (wt/vol) bovine serum albumin (Sigma) in PBS supplemented with 0.05% (vol/vol) Tween 20 (Sigma) and then probed with mouse antibodies specific for Hsp60 (66), followed by probing with CT665- or CT666-specific antibodies. Hsp60 was visualized by probing with appropriate Alexa Fluor 594-conjugated secondary antibodies, whereas CT665 and CT666 were detected with Alexa Fluor 488-conjugated antibodies (Invitrogen). Images were acquired by epifluorescence microscopy using a ×60 Apochromat objective lens on a TE2000U inverted photomicroscope (Nikon) equipped with a Retiga EXi 1394, 12-bit monochrome charge-coupled device camera and MetaMorph imaging software. Samples were prepared for immunoelectron microscopy by adsorbing Renografin-purified *C. trachomatis* serovar L2 EBs on Formvar carbon-coated copper grids and blocking by incubation with 1% (wt/vol) ovalbumin in 10 mM glycine (pH 7.4) for 5 min at room temperature. Next, grids were incubated with either α-cdsF or preimmune sera for 40 min at 37°C and washed three times with PBS. Grids were then incubated with goat anti-rabbit conjugated to either 5- or 15-nm colloidal gold (Amersham) for 40 min at 37°C, followed by three washes in PBS and three washes in distilled H_2O at room temperature. Samples were negatively stained with 2% phosphotungstic acid and washed three times in distilled H_2O for a light stain. For a heavy stain, samples were again treated with 2% phosphotungstic acid and dried without washing. Grids were viewed by using a Philips Tecnai-10 electron microscope operated at an accelerating voltage of 80 kV. All micrographs were processed by using Adobe Photoshop 6.0 (Adobe Systems).

Biochemical cross-linking studies. Proteins were covalently cross-linked in either intact cultures or free bacteria by the addition of either bismaleimidohexane (BMH) or 1,8-bis-maleimidotiethyleneglycerol ($BM[PEO]_3$; both from Pierce). For whole-culture analysis, HeLa cells were seeded in six-well cluster dishes and either infected with *C. trachomatis* L2 at a multiplicity of infection (MOI) of 1 or mock treated. Media were removed from whole cultures at ca. 20 h postinfection and replaced with 1.0 ml of HBSS. Cross-linking of free chlamydiae was performed by incubation of either intact or lysed density gradient purified *C. trachomatis* L2 EBs suspended in HBSS. For lysis, EBs were first treated for 15 min on ice with 5 mM dithiothreitol and then subjected to vigorous sonication. Similarly, logarithmic cultures of *E. coli* expressing chlamydial proteins were harvested by centrifugation and suspended in HBSS. In all cases, cross-linking reactions were carried out in 1.0-ml volumes for 30 min at ambient temperature by the addition of respective cross-linking reagent to a 3 mM final concentration (from a 100 mM stock dissolved in dimethyl sulfoxide [DMSO]) or an equivalent volume of DMSO as a mock control. Reactions were quenched by thorough washing with RPMI plus 10% fetal bovine serum, washed with HBSS, and subsequently processed for immunoblot analysis.

Yeast two and three-hybrid studies. Gateway Technology (Invitrogen) was used according to the manufacturer's guidelines to generate yeast two-hybrid constructs pDEST32-CdsE, pDEST32-CdsF, pDEST32-CdsG, pDEST22-CdsE, pDEST22-CdsF, and pDEST22-CdsG. CT665, CT666, and CT667 were amplified from chlamydial DNA using primers containing *att*B sites and mobilized into the pDONR221 vector by BP recombination reactions. Subsequent LR recombination reactions transferred CT665, CT666, and CT667 to both pDEST32 and pDEST22 yeast two-hybrid vectors containing the Gal4 DNA-binding domain (BD) and activation domain (AD), respectively. Protein-protein interactions were investigated by using the ProQuest two-hybrid system (Invitrogen) according to the manufacturer's instructions. Briefly, constructs were cotransformed into yeast strain MaV203 (Invitrogen) by using the *S.c.* EasyComp transformation kit. Transformants were selected on synthetic complete (SC) plates lacking Leu and Trp. To test for interactions, transformants were subsequently transferred onto high-stringency quadruple dropout (QDO) medium (lacking Leu, Trp, Ura, and His) with the aid of a replica plater, sterile velveteen squares (Sigma), and Whatman round filter paper (Whatman, Maidstone, United Kingdom). Plates were incubated at 30°C for up to 10 days, after which little to no growth was considered a negative result. Positive and negative controls were supplied with the kit and were used in pairs of pEXP32-Krev1 plus pEXP22-RalGDS-wt (positive) and pDEST32-Empty plus pDEST22-Empty (negative). For three-hybrid studies, MaV203 containing constructs pDEST32-CdsG plus pDEST22-CdsF and pDEST32-CdsF plus pDEST22-CdsG were made competent by using the *S.c.* EasyComp transformation kit and transformed with pY3HCdsE. Transformants were plated on vector selective medium (SC lacking Leu, Trp, and Ura) and subsequently transferred as described above to QDO plates to screen for interaction.

RESULTS

Bioinformatic evidence that CT666 encodes the *C. trachomatis* needle subunit protein. The genetic arrangement of the chlamydial T3SS is unique since apparent T3SS apparatus genes are not encoded in one pathogenicity island but are instead dispersed throughout the genome in at least four loci. Needle component proteins are small and typically located within operons encoding components of the T3SS apparatus. We, therefore, searched for small hypothetical genes located in close proximity to, or within T3SS gene clusters. The small hypothetical open reading frame (ORF) CT666 is located within an operon encoding other putative structural components of the T3SS apparatus, raising the possibility that its function is type III related. In other systems, the needle-encoding gene is flanked by two small genes encoding the needle-specific chaperones and is preceded by a conserved protein termed YscD in *Yersinia*. The *Yersinia* gene order *yscDEFG* is also apparently conserved in *C. trachomatis* since the product of ORF CT664 contains a YscD domain. We predict the ORFs CT665 and CT667 encode the needle chaperones CdsE and CdsG, respectively, since CT665 is similar in predicted mass and structure to YscE and CT667 contains tetratricopeptide repeat (TPR) domains common in class II type III-associated chaperones (Fig. 1A).

PSI-BLAST analysis (1) of CT666 failed to identify any significant sequence similarity with nonchlamydial proteins or other T3SS needle components. However, CT666 is highly conserved (>95% identity) within all *Chlamydia* spp., indicating an essential basic function. Despite this lack of primary sequence identity, CT666 does have features common to T3SS needle proteins. Like characterized needle proteins such as MxiH (pI = 4.47), CT666 has a calculated acidic pI (4.48). CT666 is similar in size to other needle proteins at 83 amino acids in length and with a predicted molecular mass of 9.14 kDa. This compares with needle proteins ranging from 73 residues in length (8.12 kDa) for *E. coli* EscF to 88 residues in length (9.5 kDa) for *Bordetella* BscF. PSI-PRED analysis (29, 39) of the predicted secondary structure of CT666 indicates that, like characterized needle proteins, CT666 is helical, com-

Downloaded from http://jb.asm.org/ on September 23, 2019 by guest

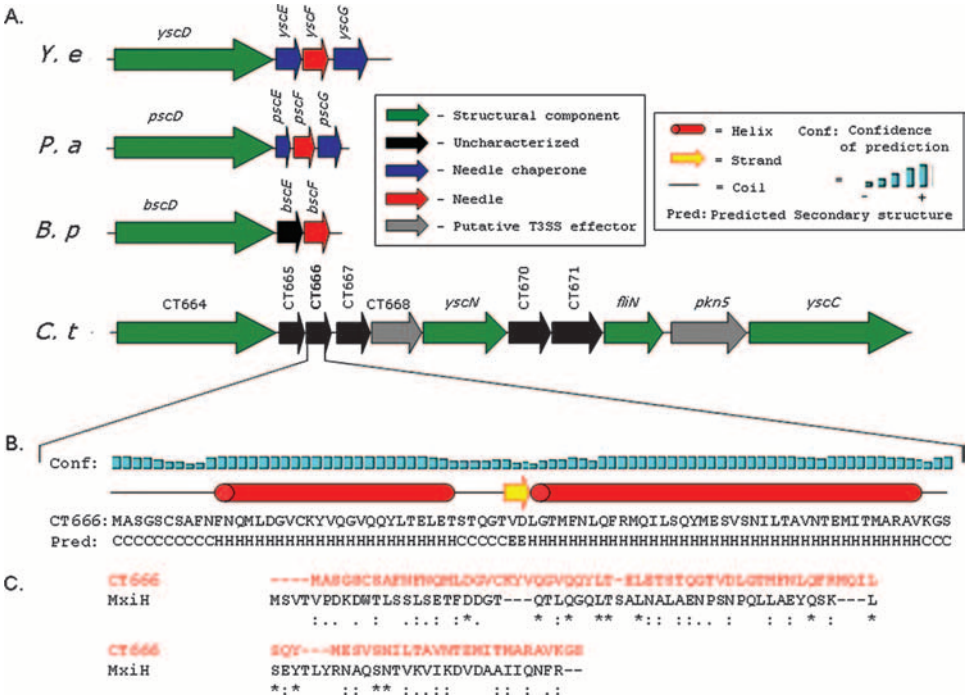

FIG. 1. Bioinformatic analysis of CdsF. (A) CT666 encoding CdsF is located in a T3SS gene cluster containing other components of the secretion system apparatus. The gene order *sctDEFG* is conserved with *Yersinia enterocolitica* (*Y.e*), *Pseudomonas aeruginosa* (*P.a*), and *Bordetella parapertussis* (*B.p*). (B) PSI-PRED analysis of the predicted secondary structure of CdsF suggests with a high level of confidence that CdsF is helical, comprising two helices connected by a loop region. (C) CLUTALW alignment of CdsF with MxiH.

prising two helices connected by a loop region (Fig. 1B). The analysis also predicts that the C-terminal helix has an extended conformation that is highly reminiscent of the MxiH structure (11, 12). Based on these predictions and in accordance with current chlamydial T3SS nomenclature, we tentatively designated CT666 as CdsF (for contact-dependent secretion protein F) (26).

CdsF is concentrated in the outer membrane complex of EBs. We next sought to experimentally test our hypothesis that CT666 indeed encodes the chlamydial T3SS needle protein. EBs contain preassembled T3SS apparatus which, via an undetermined mechanism, become secretion competent upon host-cell contact (18). Based on other T3SSs, we reasoned that the needle protein should be concentrated in the outer membrane of EBs. Therefore, we began further characterization of CdsF via Sarkosyl purification of COMCs from density gradient-purified *C. trachomatis* serovar L2 EBs. The Sarkosyl-extracted material was precipitated with trichloroacetic acid and resolved on SDS–4 to 20% PAGE gels. Staining with Coomassie brilliant blue was used initially to demonstrate that the extracted material had a protein profile typical of COMCs in accordance with the findings of Caldwell et al. (4) (Fig. 2A).

Immunoblot assays were subsequently used for further analysis of the extracted material. Samples of whole cells and Sarkosyl-soluble and -insoluble material were resolved as described above, transferred to nitrocellulose membrane, and probed with affinity-purified antibodies to MOMP, CdsC, CopN, CdsJ, and CdsF (Fig. 2B). Consistent with their functions as the major outer membrane protein and the outer membrane component of T3SS, MOMP and CdsC, respectively, were present only in the Sarkosyl-insoluble fraction. As expected, CopN, a secreted component of the T3SS, was exclusively localized in the soluble cytoplasmic fraction. CdsJ, a structural component of the T3SS spanning the periplasm, was predominantly present in the soluble fraction, although a small

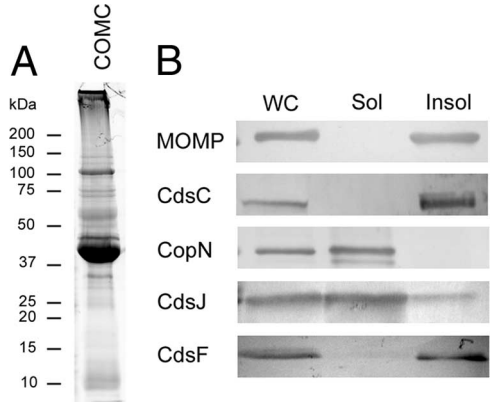

FIG. 2. Protein localization analysis of *C. trachomatis* COMCs. COMCs were harvested from density-gradient-purified EBs and SDS-PAGE resolved proteins were analyzed by Coomassie blue stain (A) or with specific antibodies via immunoblotting (B). For immunoblots, material from a *C. trachomatis* L2-infected HeLa culture (WC) was resolved as antibody specificity controls. EB-specific COMC and non-COMC protein content was tested in Sarkosyl-soluble (Sol) and -insoluble (Insol) material, respectively. Proteins were visualized by probing with secondary antibodies conjugated to alkaline phosphatase and development with NBT-BCIP.

Downloaded from http://jb.asm.org/ on September 23, 2019 by guest

amount was identified in the outer membrane portion. Although a small amount of CdsF was detected in Sarkosyl-soluble material, the majority of CdsF was detected in the insoluble material, indicating that it is specifically concentrated in the outer membrane. These results are consistent with the location of a preformed needle.

CdsF localization by immunoelectron microscopy. We first used immunoelectron microscopy to more precisely characterize the localization of CdsF in EBs. *C. trachomatis* L2 EBs were fixed, blocked with 1% ovalbumin in 10 mM glycine, and probed with affinity-purified CdsF specific antibodies or protein A-purified antibodies from preimmune serum (negative control). Sites of primary antibody reactivity were detected by incubation with second affinity antibodies conjugated to 15- or 5-nm gold particles. The localization of the gold-conjugated antibodies in relation to EBs for each sample was visualized by using electron microscopy (Fig. 3). As expected, EBs probed with preimmune sera showed no specific antibody localization (Fig. 3A). In contrast, EBs probed with antibodies specific to CdsF displayed discreet localization of gold particles at the periphery of EBs (Fig. 3B to F). Although labeling with 15-nm gold particles followed by light counterstaining revealed general CdsF surface localization (Fig. 3B), it was not efficacious for visualization of finer structures. However, localization could be seen in more detail when the second affinity antibody was conjugated to 5-nm gold particles (Fig. 3C to F). Under these conditions, anti-CdsF aggregated on the surface of filamentous-like structures reminiscent of the spike-like projections originally identified by Matsumoto et al. (33).

Next, we wanted to examine CdsF localization during infection by indirect immunofluorescence microscopy. HeLa monolayers cultivated on glass coverslips were infected with *C. trachomatis* L2 to an MOI of 1 and methanol fixed at 18 h postinfection. Coverslips were probed with mouse antibodies generated against Hsp60 to localize chlamydiae (shown in red), followed by antibodies specific to either CT665 or CdsF (shown in green), and then examined by epifluorescence microscopy (Fig. 4). The merged images demonstrate that CT665 colocalizes with Hsp60 (Fig. 4, top row), a finding consistent with its predicted role as a cytosolic protein. In contrast, CdsF distribution was most prominently observed as a rim-like staining pattern consistent with inclusion membrane localization. We observed that this inclusion membrane staining typically exhibited a punctate pattern exterior to, but in close association with, intra-inclusion-localized chlamydiae. A comparatively weak CdsF-specific signal was also detected that colocalized with Hsp60-specific staining. Both CdsF staining patterns were successfully inhibited by addition of exogenous GST-CdsF protein during primary antibody incubations (data not shown). Collectively, these data indicate that CdsF is predominantly surface localized in EBs, which is consistent with the immuno-transmission electron microscopy data, but may be inserted into the inclusion membrane during infection (Fig. 4, lower row).

Biochemical cross-linking assays demonstrate that CdsF is able to polymerize. One hallmark of needle-component proteins is their ability to self-associate and polymerize into ordered filament structures. Cross-linking assays have previously been used to investigate potential needle protein polymerization (9, 14, 60). We applied this methodology to investigate

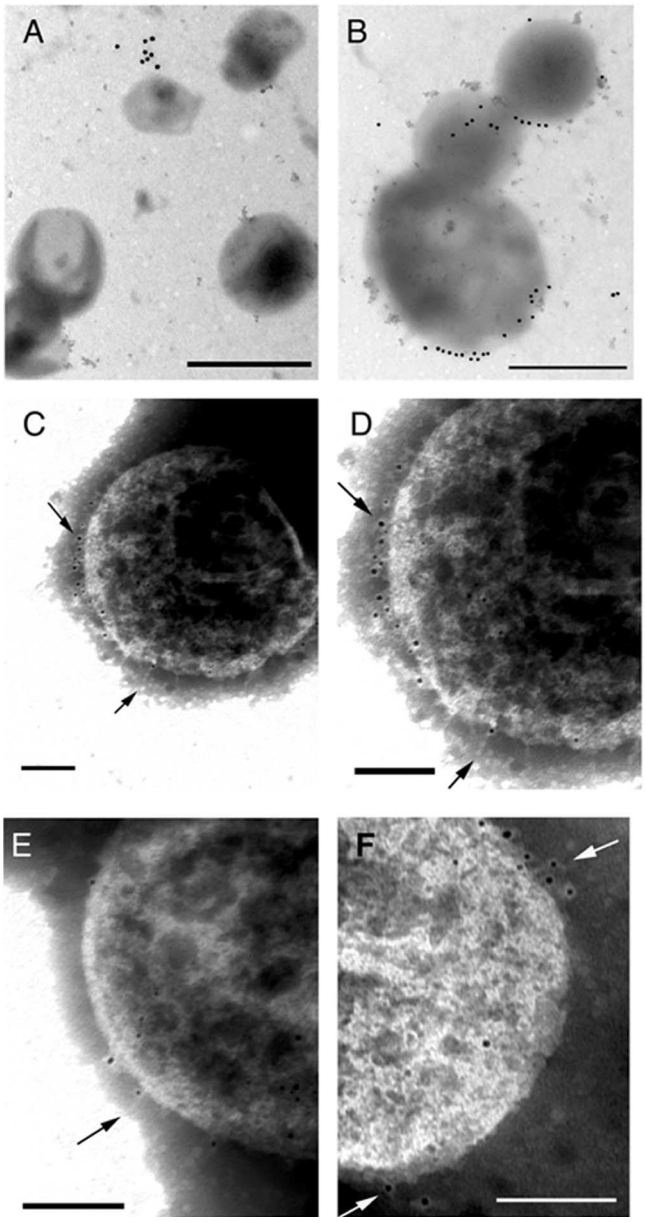

FIG. 3. Immunoelectron microscopy analysis of CdsF localization. Grid-adsorbed *C. trachomatis* L2 EBs were methanol fixed, blocked, and probed with affinity-purified CdsF-specific antibodies (B, C, D, E, and F) or protein A-purified antibodies from preimmune serum as a negative control (A). Secondary antibodies conjugated to 15 nm (A and B) or 5 nm (C to F) gold particles were used to detect sites of primary antibody reactivity. Chlamydiae were negatively counterstained by incubation with phosphotungstic acid. Representative micrographs are shown. Bars: 500 nm (A and B) or 100 nm (C to F).

CdsF's potential for polymerization during infection. HeLa monolayers were mock infected or infected with *C. trachomatis* L2 to an MOI of ca 5. At 20 h postinfection, intact culture media were treated with HBSS containing either DMSO (mock) or either a 1 or a 3 mM concentration of the covalent cross-linker BMH. After 30 min, the remaining cross-linker was quenched with 5 mM dithiothreitol, whole-culture proteins were concentrated, and CdsF was detected by immunoblotting

Downloaded from http://jb.asm.org/ on September 23, 2019 by guest

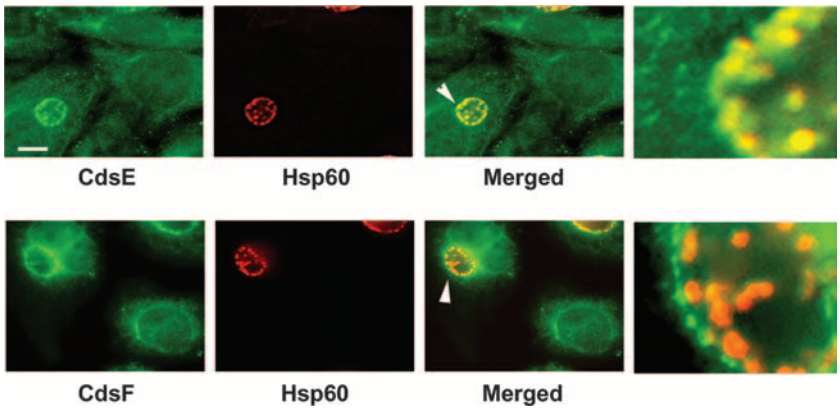

FIG. 4. Immunolocalization of CdsF during chlamydial infection. CdsF and CT665 localization was detected by indirect immunofluorescence in *C. trachomatis* L2-infected HeLa cultures infected at an MOI of 1 and cultivated at 37°C for 18 h. Hsp60 staining (red) with α-Hsp60 was used to localize chlamydiae, and cultures were probed with either α-665 or α-CdsF (both shown in green). Individual channel and merged images are shown. Arrows indicate areas of respective inclusions shown in enlarged images. Proteins were visualized by probing with Alexa 594-conjugated (for Hsp60) or Alexa 488-conjugated (for CT665 and CdsF) secondary antibodies. Bar, 5 μm.

of SDS-PAGE-resolved material (Fig. 5). CdsF was detected in an apparent monomeric form migrating at ca. 9 kDa in *C. trachomatis*-infected, DMSO-treated material. However, a monomer-sized product was only faintly detected in the presence of BMH (regardless of final concentration). Instead, at least 13 CdsF-containing bands were detected in a laddered pattern that was most apparent in the range of 30 kDa to more than 100 kDa. CdsF-reactive bands increased sequentially in apparent mass by the size of approximately one CdsF monomer. This profile is consistent with protein polymerization and is reminiscent of other needle protein profiles after biochemical cross-linking.

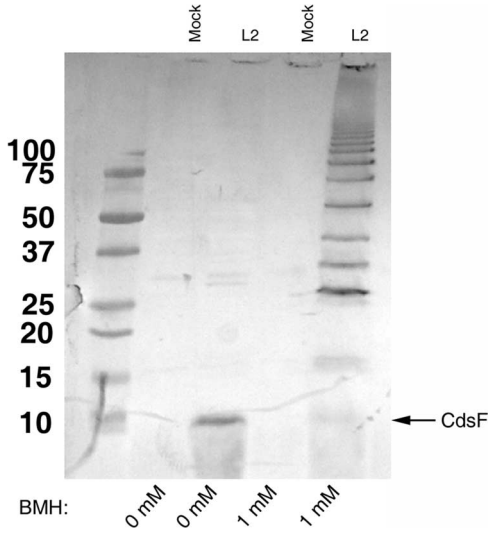

FIG. 5. Biochemical cross-linking analysis of CdsF protein-protein interactions. HeLa monolayers were mock infected or infected with *C. trachomatis* L2 at an MOI of ca. 5. Proteins were covalently modified in intact cultures after 20 h of cultivation at 37°C by addition of DMSO (0 mM, as a mock control) or BMH added to a 1 mM final concentration. Whole-culture material was harvested and concentrated, and CdsF was detected in SDS-PAGE-resolved samples via immunoblotting with CdsF-specific antibodies. Proteins were visualized by probing with secondary antibodies conjugated to alkaline phosphatase and development with NBT-BCIP.

CdsF polymerization occurs exclusively at the cell surface. Due to its solubility in DMSO, BMH is membrane permeable and, therefore, cannot be used to demonstrate that CdsF polymerization only occurs on the cell surface. To confirm that CdsF polymerization is exclusive to the exterior of the cell, we used a membrane-impermeable analog of BMH, $BM[PEO]_3$, and compared the CdsF cross-linking profile with BMH-exposed EBs. Intact or sonicated (lysed) density gradient purified *C. trachomatis* L2 EBs was either mock treated (by the addition of DMSO) or treated with 1 mM BMH or 1 mM $BM[PEO]_3$. Concentrated material was resolved on SDS–4 to 20% PAGE gradient gels and analyzed by immunoblotting with antibodies specific to CdsF or, as a control, antibodies specific to the T3SS chaperone Scc1 (Fig. 6). The CdsF cross-linking profiles of the intact EBs were essentially identical for both cross-linkers (Fig. 6A). This observation confirms that CdsF only polymerizes on the cell surface since $BM[PEO]_3$ should not have access to the bacterial cytosol. As a control, we probed the same samples with antibodies to the cytoplasmic chaperone Scc1 to ensure the envelope impermeability of intact EBs to $BM[PEO]_3$. In this case, we observed Scc1-containing cross-linked products in the presence of BMH or only when lysed material treated with $BM[PEO]_3$ (Fig. 6B). Although we do not know the full contents of these products, their absence from material from the sample treated with $BM[PEO]_3$ indicated that this cross-linker did not gain access to the EB cytoplasm. Hence, the pool of CdsF yielding the laddered profile detected in immunoblots must be localized in or on the chlamydial envelope.

CT665 and CT667 interact with each other and together with CdsF. Considering its propensity for polymerization, and by analogy to other T3SSs, CdsF is likely to require at least one chaperone to ensure soluble pools of protein prior to secretion. Earlier we highlighted the requirement of *Yersinia* and *Pseudomonas* needle proteins for the chaperones YscE/YscG and PscE/PscG. This, in addition to the apparent conservation of *CT664/665/cdsF/667* gene order with *yscDEFG*, led us to spec-

Downloaded from http://jb.asm.org/ on September 23, 2019 by guest

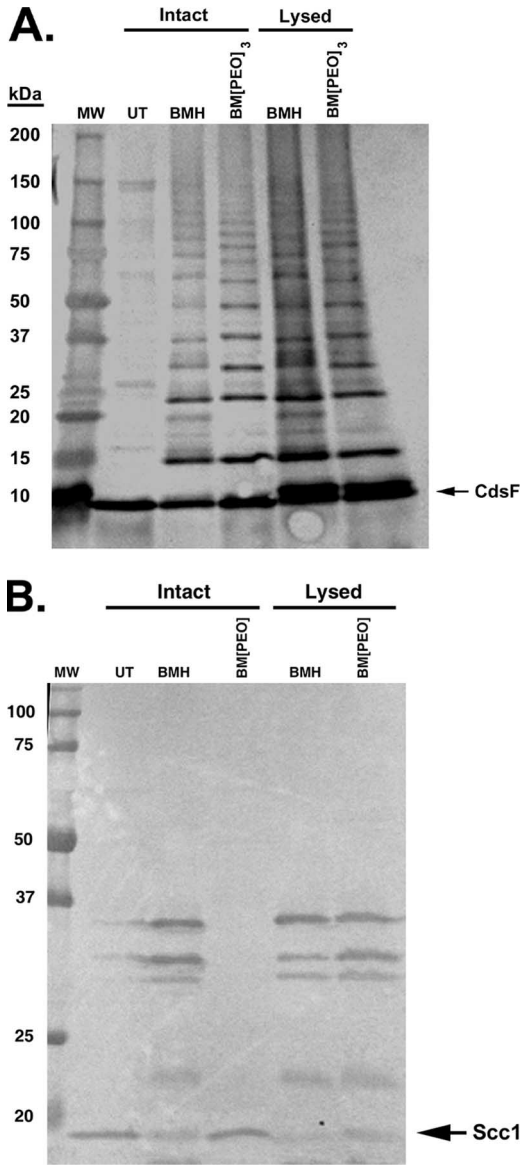

FIG. 6. Surface exposure of CdsF-containing multimers. Equal numbers of purified *C. trachomatis* L2 EBs were maintain whole (Intact) or disrupted via sonication (Lysed). Intact material was treated with DMSO as a mock control (UT). Whole-cell proteins or surface-accessible proteins were cross-linked by the addition of membrane-permeable BMH or membrane-impermeable $BM[PEO]_3$, respectively. Trichloroacetic acid-concentrated material was resolved via SDS-PAGE, and CdsF (A) or Scc1 (B) was detected with specific antibodies. Arrows indicate the position of monomer forms of each protein. Proteins were visualized by probing with secondary antibodies conjugated to alkaline phosphatase and development with NBT-BCIP.

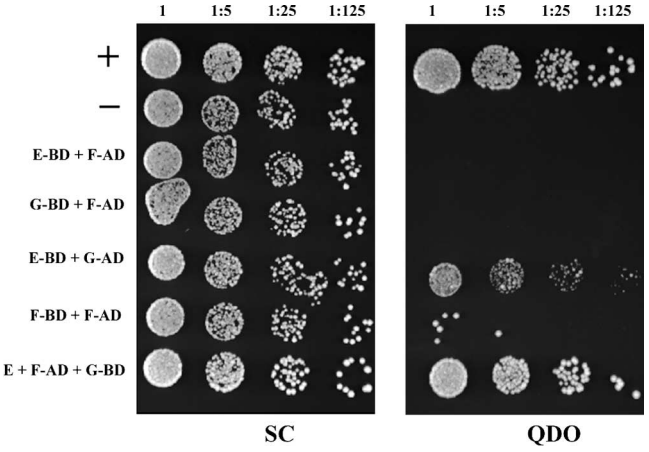

FIG. 7. Yeast two- and three-hyrbid analyses of potential CdsE-CdsF-CdsG interactions. Constructs were fused to the BD or AD of the GAL4 transcription factor. Construct pY3HCdsE expresses native CdsE lacking a fusion partner. *S. cerevisiae* MaV203 expressing either pEXP32-Krev1 plus pEXP22-RalGDS-wt as a positive control (+), pDEST32-Empty plus pDEST22-Empty as a negative control (−), pDEST32-CdsE plus pDEST22-CdsF (E-BD+F-AD), pDEST32-CdsG plus pDEST22-CdsF (G-BD+F-AD), pDEST32-CdsE plus pDEST22-CdsG (E-BD+G-AD), pDEST32-CdsF plus pDEST22-CdsF (F-BD+F-AD), or pDEST22-CdsF plus pDEST32-CdsG plus pY3HCdsE (E+F-AD+G-BD) were grown to logarithmic phase in liquid SC medium. Equal numbers of cells were harvested, subjected to fivefold serial dilution, and plated in equal amounts onto both vector-selective medium (SC) and high-stringency selective medium (QDO).

ulate that CT665 and CT667 may encode the CdsF chaperones termed CdsE and CdsG, respectively.

To investigate potential CdsE-CdsF-CdsG interactions, we used the ProQuest yeast two-hybrid system (Invitrogen). CdsE, CdsF, and CdsG were each fused to the BD and AD of the yeast two-hybrid vectors pDEST32 and pDEST22 (Invitrogen), respectively. No autoactivation of reporter genes was apparent when constructs were coexpressed with the corresponding empty vector in yeast strain *S. cerevisiae* MaV203. Protein-protein interactions between CdsE-CdsF, CdsG-CdsF, CdsE-CdsG, CdsF itself, and CdsE-CdsF-CdsG were investigated via cultivation of strains expressing pDEST32-CdsE plus pDEST22-CdsF, pDEST32-CdsG plus pDEST22-CdsF, pDEST32-CdsE plus pDEST22-CdsG, pDEST22-CdsF plus pDEST32-CdsF, or pY3HCdsE plus pDEST22-CdsF plus pDEST32-CdsG in MaV203 on either vector-selective (SC) or high-stringency (QDO) medium (Fig. 7). All strains grew equally well on SC medium. No growth of strains expressing CdsE and CdsF or CdsG and CdsF was observed even after 10 days incubation at 30°C on QDO medium. However, CdsE and CdsG expression resulted in moderate growth on selective medium. Interestingly, colonies were detected on selective medium when yeast expressed CdsF as both an AD and BD fusion, indicating that CdsF can interact with itself. Although the interaction was comparatively weak, our ability to detect growth on selective medium was reproducible. Finally, yeast containing CdsE, CdsF, and CdsG grew similarly to the positive control on selective medium. Repetition of the assay with the same pairings but with constructs in the opposite BD and AD orientations produced identical results (data not show). Taken together, the yeast two- and three-hybrid assays provide evidence that CdsE and CdsG interact with each other and that both chaperones are required for interaction with CdsF.

CdsE and CdsG are required for CdsF stability. Needle chaperones bind to needle subunits in the bacterial cytosol to prevent the physiologically unfavorable process of premature polymerization. In the absence of respective chaperones, needle proteins are rapidly degraded (8, 40, 41). We therefore chose to investigate potential functional implications of the

Downloaded from http://jb.asm.org/ on September 23, 2019 by guest

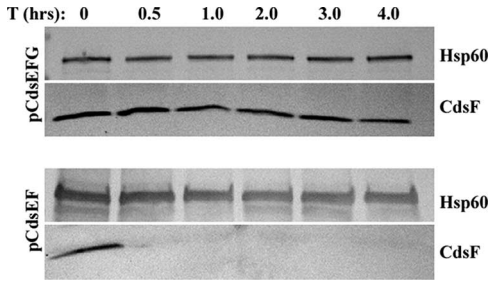

FIG. 8. Coexpression of CdsE and CdsG promotes CdsF stability. Log-phase *E. coli* cultures expressing pCdsEF or pCdsEFG were supplemented with chloramphenicol to halt de novo protein synthesis. Proteins were concentrated from whole culture samples removed 0 min, 30 min, 1 h, 2 h, 3 h, and 4 h after antibiotic addition. Material corresponding to 0.01 OD · ml of CdsEFG or 0.10 OD.ml of CdsEF-expressing cultures were resolved via SDS-PAGE and probed in immunoblots with α-CdsF and α-Hsp60. Proteins were visualized by probing with secondary antibodies conjugated to alkaline phosphatase and development with NBT-BCIP.

CdsE-CdsF-CdsG interaction by examining the levels of ectopically expressed CdsF in the presence or absence of a functional chaperone pair (Fig. 8). Native CdsF was expressed in *E. coli* from either pCdsEFG-FT, where all three proteins are produced, or from pCdsEF, which lacks CdsG. Cultures were supplemented with chloramphenicol to inhibit de novo protein synthesis, and CdsF abundance was examined by immunoblotting of material harvested at various times after antibiotic addition. In the presence of CdsE and CdsG, CdsF was detectable in roughly equal amounts at all times. In contrast, we only observed CdsF in time zero (lane 1) material when CdsG was deleted. We probed immunoblots for endogenous *E. coli* Hsp60 as an internal loading control and, as expected, this protein was present in all material. Expression of native CdsF alone yielded results similar to those seen for CdsEF (data not shown). These data indicate that CdsF is rapidly degraded by *E. coli* in the absence of both CdsE and CdsG and that the functional significance of the tripartite interaction is to protect cytoplasmic pools of CdsF. Although we cannot provide definitive evidence, it is likely that CdsE and CdsG serve as chaperones for native CdsF prior to its secretion by chlamydiae.

DISCUSSION

Multiple groups have provided microscopic evidence that *Chlamydia* spp. possess surface-localized, filamentous projections. These structures are very reminiscent of T3SS-associated needle structures that are required for the delivery of T3SS effector proteins (in conjunction with additional "translocator" proteins), presumably by bridging the gap between the bacterial envelope and an intimately associated eukaryotic membrane (19). Evidence from other T3SSs indicates that these extended filaments consist of a single protein, and yet a homolog is not readily apparent in chlamydial genomes. We began an in silico search for the chlamydial needle ortholog by focusing on the locus flanked by genes for the predicted T3SS-associated chaperone CT663 and the outer membrane secretin CdsC (CT674). This locus contains a hypothetical ORF (CT666) predicted to encode a protein of correct physiochemical parameters. Moreover, the other genes of this locus are arranged in operons (24) and predicted to encode important members of the T3SS apparatus, including the ATPase, chaperones, and membrane components (16). There is evidence that CT668, CT670, and CT671 are secreted proteins (47, 51), and yet given their gene order they could represent mobile components of the T3SS apparatus. Indeed, CT670 contains an YscO-like domain raising the possibility that CT670 and CT671 correspond to the secreted *Yersinia* apparatus components YscO and YscP, respectively.

Despite the lack of highly conserved primary sequences outside of *Chlamydia*, we have noted many features of CdsF common to needle proteins (Fig. 1). The initial failure of broad database homology searches may be due to the small size of this group of proteins and the fact that known needle proteins among T3SSs only display 20 to 30% sequence identity (12). Indeed, direct alignment of CdsF with *S. flexneri* MxiH using CLUSTAL W (59) does reveal 57.8% overall similarity (Fig. 1C). CdsF does lack the P-(S/D)-(D/N)-P turn, a four-residue ordered-loop region conserved among many other characterized needle proteins (12, 30, 61). However, this conservation is not complete, and the motif is only partially present, for example, in EscF of *E. coli*, PscF of *Pseudomonas* spp., and SsaH from *Salmonella* SPI-2 (63). Moreover, CdsF does contain the adjacent conserved glutamine residue at position 49 that has been shown to be essential for function of *Yersinia* YscF (60).

Our biochemical and microscopy data support bioinformatic indications that CdsF represents the *C. trachomatis* needle protein. CdsF copurifies with outer membrane complexes and can be localized via immunoelectron microscopy to spikelike projections on the surface of EBs. CdsF appears to be secreted by chlamydiae and gains access to the inclusion membrane during infection (Fig. 4). We could not detect CdsF-specific signal in the host cytoplasm, and yet due to the cross-reactivity of the antibodies with the host, we cannot exclude the possibility that small amounts of CdsF reach the cytosol. Biochemical cross-linking assays provided additional evidence that CdsF represents the chlamydial needle protein by showing that CdsF polymerizes during infection and that this occurs exclusively on the surface of EBs. Although we have not formally excluded the possibility that cross-linked products may contain other proteins, evidence indicates that the laddering pattern contains only CdsF. The reactive ladder of bands increases by the size of approximately one CdsF monomer, and CdsF was found to interact with itself in yeast two-hybrid studies.

Interestingly, cross-linking assays revealed a subtle difference in CdsF band patterns. When cross-linking was performed on intact cultures in which the RB developmental form dominated, the first dominant cross-linked product appeared to correlate with the size of trimeric CdsF (Fig. 5, lane 5). Conversely, a cross-linked product corresponding to dimeric CdsF is clearly detected when EBs were treated (Fig. 6A, lanes 3 and 4). Significant amounts of the monomer were also detected in EBs. Monomer could correspond to a pool of unpolymerized CdsF in the bacterial cytoplasm since we did detect some CdsF in Sarkosyl-soluble fractions (Fig. 2). However, it could also correspond to a needle conformation that is less efficiently cross-linked in EBs. Collectively, these observations may have significance relating to the functional form of the needle. The needle plays a direct role in host-cell detection, mediating the activation of secretion by transmission of an

Downloaded from http://jb.asm.org/ on September 23, 2019 by guest

"activation signal" upon host cell contact (30, 60). The precise mechanism by which this occurs has not yet been elucidated; however, it has been postulated that a conformational change in the helical arrangement of the needle may be responsible (30). Hence, the detection of CdsF trimers or dimers could reflect an alteration in helical assembly.

Alternatively, Cordes et al. (6) reported that MxiH mutants affecting secretion activity do not change helical packing. In this case, the alteration in cross-linking pattern could correspond to states in which CdsF is interacting with different proteins. For example, CdsF likely interacts with translocator proteins embedded in the inclusion membrane in the context of a native infection, whereas in EBs it could interact with capping proteins similar to those described for *Shigella* or *Yersinia* needles (13, 41). Regardless of the mechanism, it is therefore probable that the different dominant bands seen here in the cross-linking ladders during active T3S (RBs) and inactive T3S (EBs) represent an alteration in the functional state CdsF.

Another interesting aspect regarding our cross-linking data is that we were able to use the homobifunctional, sulfhydryl-reactive cross-linker BMH. Other than the single Cys residue in the *Salmonella* SPI-2 protein SsaH, no other needle proteins contain Cys residues. This makes CdsF somewhat unique with its two cysteines at positions 6 and 19. Given the correlation between the chlamydial developmental cycle and the degree of disulfide bonds in cysteine-rich proteins of the chlamydial envelope (23), it is tempting to speculate that the unique Cys residues found in CdsF provide a link between T3SS activity and chlamydial development. The ability of BMH to gain access to these N-terminally localized residues may have significance in defining the overall conformation of needle class proteins. Cys-9 is located within a predicted coil, whereas Cys-19 lies within a helix predicted to be buried within a polymerized needle. Predictions of surface exposure are difficult since the N terminus of MxiH is disordered, and yet MxiH models predict that the N terminus forms an inner structure surrounded by the C termini of other monomers in a polymerized needle (11). However, the N terminus of both MxiH and CdsF contain hydrophilic residues that are presumably either exposed to solvent or involved in intramolecular interactions within the packed structure. Further testing will be required to delineate the orientation of these residues to the exterior or interior of the needle. We favor a model in which these residues are exposed to the exterior, since it is difficult to envision BMH gaining access to the needle channel.

In addition to characterizing CdsF, we have also provided evidence that CT665 and CT667 encode the needle chaperones CdsE and CdsG, respectively. The recently resolved crystal structure of the *Pseudomonas* PscE-PscF-PcsG complex reveals that PscE is a small helical protein consisting of two antiparallel helices that are preceded by a short helix (45). *Chlamydia* CdsE is similar in size to PscE and is predicted to comprise at least two helices (data not shown). Interestingly, CdsE and CdsF, like PscE and PscF, share a similar size and predicted secondary structure. Consistent with results obtained for PscE, our immunofluorescence data indicated that this protein was not secreted by chlamydiae, and cross-linking assays failed to detect CdsE multimerization (data not shown). *Pseudomonas* PscG consists of an array of three TPR-like motifs reminiscent of the predicted structure of class II T3SS chaperones (43, 45). PSI-PRED predicted secondary structure of *Chlamydia* CdsG reveals that, like PscG, the protein likely comprises seven helices incorporating three TPR arrays. In the PscE-PscF-PscG complex, PscE interacts with and stabilizes PscG, while PscG directly interacts with the amphipathic C-terminal tail of PcsF, thereby preventing degradation and polymerization of PscF in the bacterial cytosol. Using a yeast two- and three-hybrid assay for protein-protein interactions, we found that, similar to the situation in *Pseudomonas*, CdsE and CdsG interacted, and yet a CdsF-CdsG interaction was only detectable in the presence of CdsE. Due to the genetic intractability of *Chlamydia*, we were unable to directly investigate the consequences of the CdsE-CdsF-CdsG complex during infection. However, we were able to demonstrate a functional consequence of the interaction using *E. coli* as a surrogate host. These data are consistent with a role of the chaperones in binding CdsF to prevent premature turnover in the bacterial cytoplasm.

In summary, we have provided evidence that CT666 encodes the T3SS needle protein CdsF in the globally significant pathogen *Chlamydia*. Currently, antibiotics are successfully used to treat all types of chlamydial infection. However, treatment may not always be available, rates of reinfection can be high, and a significant proportion of urogenital infections are asymptomatic until more serious disease manifestations appear (46). To circumvent these problems, the identification of potential vaccine candidates is a highly desirable goal in the field of chlamydial basic research. CdsF may represent one such candidate. The T3SS needle is known to exist as a preformed structure on the cell surface and is essential for T3SS activity in other systems. Indeed, hyperimmunization with *Yersinia* YscF has been shown to protect mice from *Y. pestis* infection (35, 54). Furthermore, CdsF is highly conserved in *Chlamydia* with >95% sequence identity between all strains, raising the possibility that a CdsF-based vaccine may provide a wide range of protection against all medically significant strains of *Chlamydia*. We are therefore currently pursuing multiple mechanisms to neutralize CdsF function.

ACKNOWLEDGMENTS

We thank Harlan Caldwell (Rocky Mountain Laboratories, National Institute of Allergy and Infectious Disease [NIAID]) for the gift of MOMP-specific antibodies. We acknowledge the expert assistance of Judy Whittimore, Electron Microscopy Core Facility in the Department of Pathology, J. H. Quillen College of Medicine, East Tennessee State University. We also thank G. Plano and K. Wolf, as well as members of the Fields laboratory for critical reading of the manuscript.

This study was supported by Public Health Service grants from the National Institutes of Health, NIAID (AI065530 for K.A.F and AI13446 for P.B.W.).

REFERENCES

1. **Altschul, S. F., T. L. Madden, A. A. Schaffer, J. Zhang, Z. Zhang, W. Miller, and D. J. Lipman.** 1997. Gapped BLAST and PSI-BLAST: a new generation of protein database search programs. Nucleic Acids Res. **25:**3389–3402.
2. **Baehr, W., Y. X. Zhang, T. Joseph, H. Su, F. E. Nano, K. D. Everett, and H. D. Caldwell.** 1988. Mapping antigenic domains expressed by *Chlamydia trachomatis* major outer membrane protein genes. Proc. Natl. Acad. Sci. USA **85:**4000–4004.
3. **Bavoil, P. M., and R. C. Hsia.** 1998. Type III secretion in *Chlamydia*: a case of deja vu? (Letter.) Mol. Microbiol. **28:**860–862.
4. **Caldwell, H. D., J. Kromhout, and J. Schachter.** 1981. Purification and partial characterization of the major outer membrane protein of *Chlamydia trachomatis*. Infect. Immun. **31:**1161–1176.
5. **Chang, J. J., K. R. Leonard, and Y. X. Zhang.** 1997. Structural studies of the

Downloaded from http://jb.asm.org/ on September 23, 2019 by guest

surface projections of *Chlamydia trachomatis* by electron microscopy. J. Med. Microbiol. **46:**1013–1018.
6. **Cordes, F. S., S. Daniall, R. Kenjale, S. Saurya, W. L. Picking, W. D. Picking, F. Booy, S. M. Lea, and A. Blocker.** 2005. Helical packing of needles from functionally altered *Shigella* type III secretion systems. J. Mol. Biol. **354:**206–211.
7. **Cordes, F. S., K. Komoriya, E. Larquet, S. Yang, E. H. Egelman, A. Blocker, and S. M. Lea.** 2003. Helical structure of the needle of the type III secretion system of *Shigella flexneri*. J. Biol. Chem. **278:**17103–17107.
8. **Darboe, N., R. Kenjale, W. L. Picking, W. D. Picking, and C. R. Middaugh.** 2006. Physical characterization of MxiH and PrgI, the needle component of the type III secretion apparatus from *Shigella* and *Salmonella*. Protein Sci. **15:**543–552.
9. **Davis, A. J., and J. Mecsas.** 2007. Mutations in the *Yersinia pseudotuberculosis* type III secretion system needle protein, YscF, that specifically abrogate effector translocation into host cells. J. Bacteriol. **189:**83–97.
10. **Day, J. B., I. Guller, and G. V. Plano.** 2000. *Yersinia pestis* YscG protein is a Syc-like chaperone that directly binds yscE. Infect. Immun. **68:**6466–6471.
11. **Deane, J. E., F. S. Cordes, P. Roversi, S. Johnson, R. Kenjale, W. D. Picking, W. L. Picking, S. M. Lea, and A. Blocker.** 2006. Expression, purification, crystallization and preliminary crystallographic analysis of MxiH, a subunit of the *Shigella flexneri* type III secretion system needle. Acta Crystallogr. Sect. F Struct. Biol. Crystallogr. Commun. **62:**302–305.
12. **Deane, J. E., P. Roversi, F. S. Cordes, S. Johnson, R. Kenjale, S. Daniall, F. Booy, W. D. Picking, W. L. Picking, A. Blocker, and S. M. Lea.** 2006. Molecular model of a type three secretion system needle: implications for host cell sensing. Proc. Natl. Acad. Sci. USA **103:**12529–12533.
13. **Espina, M., A. J. Olive, R. Kenjale, D. S. Moore, S. F. Ausar, R. W. Kaminski, E. V. Oaks, C. R. Middaugh, W. D. Picking, and W. L. Picking.** 2006. IpaD localizes to the tip of the type III secretion system needle in *Shigella flexneri*. Infect. Immun. **74:**4391–4400.
14. **Ferracci, F., F. D. Schubot, D. S. Waugh, and G. V. Plano.** 2005. Selection and characterization of *Yersinia pestis* YopN mutants that constitutively block Yop secretion. Mol. Microbiol. **57:**970–987.
15. **Fields, K. A., E. R. Fischer, D. J. Mead, and T. Hackstadt.** 2005. Analysis of putative *Chlamydia trachomatis* chaperones Scc2 and Scc3 and their use in the identification of type III secretion substrates. J. Bacteriol. **187:**6466–6478.
16. **Fields, K. A., and T. Hackstadt.** 2006. The *Chlamydia* type III secretion system: structure and implications for pathogenesis, p. 220–233. *In* P. Bavoil and P. B. Wyrick (ed.), *Chlamydia*: genomics and pathogenesis. Horizon Press, Norfolk, United Kingdom.
17. **Fields, K. A., and T. Hackstadt.** 2000. Evidence for the secretion of *Chlamydia trachomatis* CopN by a type III secretion mechanism. Mol. Microbiol. **38:**1048–1060.
18. **Fields, K. A., D. J. Mead, C. A. Dooley, and T. Hackstadt.** 2003. *Chlamydia trachomatis* type III secretion: evidence for a functional apparatus during early-cycle development. Mol. Microbiol. **48:**671–683.
19. **Galan, J. E., and H. Wolf-Watz.** 2006. Protein delivery into eukaryotic cells by type III secretion machines. Nature **444:**567–573.
20. **Ghosh, P.** 2004. Process of protein transport by the type III secretion system. Microbiol. Mol. Biol. Rev. **68:**771–795.
21. **Gophna, U., E. Ron, and D. Graur.** 2003. Bacterial type III secretion systems are ancient and evolved by multiple horizontal-transfer events. Gene **312:**151–163.
22. **Hackstadt, T., D. D. Rockey, R. A. Heinzen, and M. A. Scidmore.** 1996. *Chlamydia trachomatis* interrupts an exocytic pathway to acquire endogenously synthesized sphingomyelin in transit from the Golgi apparatus to the plasma membrane. EMBO J. **15:**964–977.
23. **Hatch, T. P., I. Allan, and J. H. Pearce.** 1984. Structural and polypeptide differences between envelopes of infective and reproductive life cycle forms of *Chlamydia* spp. J. Bacteriol. **157:**13–20.
24. **Hefty, P. S., and R. S. Stephens.** 2007. Chlamydial type III secretion system is encoded on ten operons preceded by sigma 70-like promoter elements. J. Bacteriol. **189:**198–206.
25. **Hoiczyk, E., and G. Blobel.** 2001. Polymerization of a single protein of the pathogen *Yersinia enterocolitica* into needles punctures eukaryotic cells. Proc. Natl. Acad. Sci. USA **10:**4669–4674.
26. **Hsia, R. C., Y. Pannekoek, E. Ingerowski, and P. M. Bavoil.** 1997. Type III secretion genes identify a putative virulence locus of *Chlamydia*. Mol. Microbiol. **25:**351–359.
27. **Hueck, C. J.** 1998. Type III protein secretion systems in bacterial pathogens of animals and plants. Microbiol. Mol. Biol. Rev. **62:**379–433.
28. **Hybiske, K., and R. S. Stephens.** 2007. Mechanisms of host cell exit by the intracellular bacterium *Chlamydia*. Proc. Natl. Acad. Sci. USA **104:**11430–11435.
29. **Jones, D.** 1999. Protein secondary structure prediction based on position-specific scoring matrices. J. Mol. Biol. **266:**814–830.
30. **Kenjale, R., J. Wilson, S. F. Zenk, S. Saurya, W. L. Picking, W. D. Picking, and A. Blocker.** 2005. The needle component of the type III secretion apparatus of *Shigella* regulates the activity of the secretion apparatus. J. Biol. Chem. **280:**42929–42937.
31. **Kubori, T., A. Sukhan, S. I. Aizawa, and J. E. Galan.** 2000. Molecular characterization and assembly of the needle complex of the *Salmonella typhimurium* type III protein secretion system. Proc. Natl. Acad. Sci. USA **97:**10225–10230.
32. **Laemmli, U. K.** 1970. Cleavage of structural proteins during the assembly of the head of bacteriophage T4. Nature **227:**680–685.
33. **Maniatis, T., E. F. Fritsch, and J. Sambrook.** 1982. Molecular cloning: a laboratory manual. Cold Spring Harbor Laboratory, Cold Spring Harbor, NY.
34. **Marlovits, T. C., T. Kubori, A. Sukhan, D. R. Thomas, J. E. Galan, and V. M. Unger.** 2004. Structural insights into the assembly of the type III secretion needle complex. Science **306:**1040–1042.
35. **Matson, J. S., K. A. Durick, D. S. Bradley, and M. L. Nilles.** 2005. Immunization of mice with YscF provides protection from *Yersinia pestis* infections. BMC Microbiol. **24:**38–48.
36. **Matsumoto, A.** 1981. Electron microscopic observations of surface projections and related intracellular structures of *Chlamydia* organisms. J. Electron Microsc. **30:**315–320.
37. **Matsumoto, A.** 1982. Electron microscopic observations of surface projections on *Chlamydia psittaci* reticulate bodies. J. Bacteriol. **150:**358–364.
38. **Matsumoto, A., E. Fujiwara, and N. Higashi.** 1976. Observations of the surface projections of infectious small cell of *Chlamydia psittaci* in thin sections. J. Electron Microsc. **25:**169–170.
39. **McGuffin, L., K. Bryson, and D. Jones.** 2000. The PSIPRED protein structure prediction server. Bioinformatics **16:**404–405.
40. **Moulder, J. W.** 1991. Interaction of chlamydiae and host cells in vitro. Microbiol. Rev. **55:**143–190.
41. **Mueller, C. A., P. Broz, S. A. Muller, P. Ringler, F. Erne-Brand, I. Sorg, M. Kuhn, A. Engel, and G. Cornelis.** 2005. The V-antigen of *Yersinia* forms a distinct structure at the tip of injectisome needles. Science **310:**674–676.
42. **Nichols, B. A., P. Y. Setzer, F. Pang, and C. R. Dawson.** 1985. New view of the surface projections of *Chlamydia trachomatis*. J. Bacteriol. **164:**344–349.
43. **Pallen, M. J., M. S. Francis, and K. Futterer.** 2003. Tetratricopeptide-like repeats in type III-secretion chaperones and regulators. FEMS Microbiol. Lett. **223:**53–60.
44. **Quinaud, M., J. Chabert, E. Faudry, E. Neumann, D. Lemaire, A. Pastor, S. Elsen, A. Dessen, and I. Attree.** 2005. The PscE-PscF-PscG complex controls type III secretion needle biogenesis in *Pseudomonas aeruginosa*. J. Biol. Chem. **280:**36293–36300.
45. **Quinaud, M., S. Ple, V. Job, C. Contreras-Martel, J. P. Simorre, I. Attree, and A. Dessen.** 2007. Structure of the heterotrimeric complex that regulates type III secretion needle formation. Proc. Natl. Acad. Sci. USA **104:**7803–7808.
46. **Schachter, J.** 1999. Infection and disease epidemiology, p. 139–169. *In* R. S. Stephens (ed.), *Chlamydia*: intracellular biology, pathogenesis, and immunity. ASM Press, Washington, DC.
47. **Sisko, J. L., K. Spaeth, Y. Kumar, and R. H. Valdivia.** 2006. Multifunctional analysis of *Chlamydia*-specific genes in a yeast expression system. Mol. Microbiol. **60:**51–66.
48. **Slepenkin, A., L. M. de la Maza, and E. M. Peterson.** 2005. Interaction between components of the type III secretion system of *Chlamydiaceae*. J. Bacteriol. **187:**473–479.
49. **Stokes, G. V.** 1978. Surface projections and internal structure of *Chlamydia psittaci*. J. Bacteriol. **133:**1514–1516.
50. **Subtil, A., A. Blocker, and A. Dautry-Varsat.** 2000. Type III secretion system in *Chlamydia* species: identified members and candidates. Microbes Infect. **2:**367–369.
51. **Subtil, A., C. Delevoye, M. E. Balana, L. Tastevin, S. Perrinet, and A. Dautry-Varsat.** 2005. A directed screen for chlamydial proteins secreted by a type III mechanism identifies a translocated protein and numerous other new candidates. Mol. Microbiol. **56:**1636–1647.
52. **Subtil, A., C. Parsot, and A. Dautry-Varsat.** 2001. Secretion of predicted Inc proteins of *Chlamydia pneumoniae* by a heterologous type III machinery. Mol. Microbiol. **39:**792–800.
53. **Sukhan, A., T. Kubori, and J. E. Galan.** 2003. Synthesis and localization of the *Salmonella* SPI-1 type III secretion needle complex proteins PrgI and PrgJ. J. Bacteriol. **185:**3480–3483.
54. **Swietnicki, W., B. S. Powell, and J. Goodin.** 2005. *Yersinia pestis* Yop secretion protein F: purification, characterization and protective efficacy against bubonic plague. Protein Expr. Purif. **42:**166–172.
55. **Tamano, K., S. Aizawa, E. Katayama, T. Nonaka, S. Imajoh-Ohmi, A. Kuwae, S. Nagai, and C. Sasakawa.** 2000. Supramolecular structure of the *Shigella* type III secretion machinery: the needle part is changeable in length and essential for delivery of effectors. EMBO J. **19:**3876–3887.
56. **Tamano, K., E. Katayama, T. Toyotome, and C. Sasakawa.** 2002. *Shigella* Spa32 is an essential secretory protein for functional type III secretion machinery and uniformity of its needle length. J. Bacteriol. **184:**1244–12454.
57. **Tampakaki, A. P.** 2004. Conserved features of type III secretion. Cell Microbiol. **6:**805–816.
58. **Tanzer, R. J., and T. P. Hatch.** 2001. Characterization of outer membrane proteins in *Chlamydia trachomatis* LGV serovar L2. J. Bacteriol. **183:**2686–2690.
59. **Thompson, J. D., D. G. Higgins, and T. J. Gibson.** 1994. CLUSTAL W:

Downloaded from http://jb.asm.org/ on September 23, 2019 by guest

improving the sensitivity of progressive multiple sequence alignment through sequence weighting, position-specific gap penalties, and weight matrix choice. Nucleic Acids Res. **22:**4673–4680.
60. **Torruellas, J., M. W. Jackson, J. W. Pennock, and G. V. Plano.** 2005. The *Yersinia pestis* type III secretion needle plays a role in regulation of Yop secretion. Mol. Microbiol. **57:**1719–1733.
61. **Wang, Y., A. N. Ouellette, C. W. Egan, T. Rathinavelan, W. Im, and R. N. De Guzman.** 2007. Differences in the electrostatic surfaces of the type III secretion needle proteins PrgI, BsaL, and MxiH. J. Mol. Biol. **371:**1304–1314.
62. **Wilham, G., S. Dittmann, A. Schmid, and J. Heesemann.** 2007. On the role of specific chaperones, the specific ATPase, and the proton motive force in type III secretion. Int. J. Med. Microbiol. **297:**27–36.
63. **Wilson, R. K., R. K. Shaw, S. Daniell, S. Knutton, and G. Frankel.** 2001. Role of EscF, a putative needle complex protein, in the type III protein translocation system of enteropathogenic *Escherichia coli*. Cell Microbiol. **3:**753–762.
64. **Winstanley, C., and C. A. Hart.** 2001. Type III secretion systems and pathogenicity islands. J. Med. Microbiol. **50:**116–126.
65. **Wolf, K., E. Fischer, and T. Hackstadt.** 2000. Ultrastructural analysis of developmental events in *Chlamydia pneumoniae*-infected cells. Infect. Immun. **68:**2379–2385.
66. **Yuan, Y., K. Lyng, Y. X. Zhang, D. D. Rockey, and R. P. Morrison.** 1992. Monoclonal antibodies define genus-specific, species-specific, and cross-reactive epitopes of the chlamydial 60-kilodalton heat shock protein (hsp60): specific immunodetection and purification of chlamydial hsp60. Infect. Immun. **60:**2288–2296.

Downloaded from http://jb.asm.org/ on September 23, 2019 by guest